Washington eXperimental Mathematics Lab
University of Washington
mpetta@uw.edu

Visualizing the Laplace Transform

From Differential Equations to the Complex Plane

Andrew Loveless & Michael Petta

Abstract. The Laplace transform is one of the most powerful tools in applied mathematics, converting differential equations into algebraic ones by shifting perspective from the time domain to the complex frequency domain. This project investigates how the Laplace transform can be understood visually: why the kernel e^{-st} acts as a weighted average, how poles and zeros in the complex s-plane govern the behavior of physical systems, and how a forced mass-spring oscillator decomposes naturally into transient and steady-state parts through the lens of partial fractions. Three animated visualizations were produced using the Manim animation library, building intuition from first principles through the RC circuit, the forced second-order oscillator, and a three-dimensional surface over the complex plane.

1 Introduction

Differential equations describe how physical quantities change over time. Solving them directly can be difficult, particularly when forcing terms or initial conditions complicate the algebra. The Laplace transform sidesteps these difficulties by converting a differential equation in t into an algebraic equation in the complex variable $s = \sigma + j\omega$.

The central idea is geometric: the solution in the s-plane lives on a surface $|H(s)|$ whose peaks and valleys reveal everything about the system's natural frequencies, damping, and response to external forces. This project makes that geometry visible through three videos:

1. **LaplaceTransform** – RC circuit introduction to the transform, kernel intuition, and Bode plots.

2. **ForcedMassSpringLaplace** – Second-order forced oscillator, time-domain decomposition, frequency response, and pole-zero map.

3. **LaplaceViz3D** – The full $|H(s)|$ surface over $\mathbb{C}$, four damping cases, and the three-surface decomposition.

2 The Laplace Transform

2.1 Definition

The (one-sided) Laplace transform of a function $f(t)$ is defined as

$$\mathcal{L}\{f(t)\} = F(s) = \int_0^\infty f(t)\, e^{-st}\, dt, \quad s \in \mathbb{C}. \tag{1}$$

The kernel $e^{-st} = e^{-\sigma t} e^{-j\omega t}$ combines an exponential decay (controlled by $\sigma = \mathrm{Re}(s)$) with a sinusoidal oscillation (controlled by $\omega = \mathrm{Im}(s)$). Intuitively, $F(s)$ asks: *how much of the frequency s is present in f?*

2.2 Key Transform Pairs

Table 1 lists the transform pairs used throughout this project.

Table 1: Common Laplace Transform Pairs

$f(t)$	$F(s)$
e^{-at}	$\frac{1}{s+a}$
$\sin(\omega_0 t)$	$\frac{\omega_0}{s^2+\omega_0^2}$
$\cos(\omega_0 t)$	$\frac{s}{s^2+\omega_0^2}$
$e^{-at}\cos(\omega_d t)$	$\frac{s+a}{(s+a)^2+\omega_d^2}$
$u(t)$ (unit step)	$\frac{1}{s}$
$\delta(t)$ (impulse)	1

2.3 Differentiation Rule

The key property that makes the Laplace transform useful for ODEs is

$$\mathcal{L}\{f'(t)\} = s\,F(s) - f(0^-), \tag{2}$$

which follows directly from integration by parts. Applying this twice gives

$$\mathcal{L}\{f''(t)\} = s^2 F(s) - s\,f(0^-) - f'(0^-). \tag{3}$$

Initial conditions enter naturally as algebraic terms – no special treatment required.

3 RC Circuit: A First Example

3.1 The ODE and Transfer Function

A series RC circuit with input voltage $v_{\text{in}}(t)$ and capacitor voltage $v_C(t)$ satisfies Kirchhoff's Voltage Law:

$$RC\,\frac{dv_C}{dt} + v_C = v_{\text{in}}. \tag{4}$$

Taking the Laplace transform with zero initial conditions gives

$$(1 + sRC)\,V_C(s) = V_{\text{in}}(s), \tag{5}$$

so the transfer function is

$$H(s) = \frac{V_C(s)}{V_{\text{in}}(s)} = \frac{1}{1 + sRC}. \tag{6}$$

This has a single pole at $s = -1/RC$, located in the left half of the complex plane, confirming that the circuit is stable.

3.2 Frequency Response and Bode Plot

On the imaginary axis $s = j\omega$, the magnitude is

$$|H(j\omega)| = \frac{1}{\sqrt{1 + (\omega RC)^2}}. \tag{7}$$

The $-3\,\text{dB}$ cutoff occurs at $\omega_c = 1/RC$, where the output power is halved. The step response is $v_C(t) = (1 - e^{-t/RC})\,u(t)$, reaching 63.2% of its final value at $t = \tau = RC$.

3.3 Geometric Insight

A key visual idea: the magnitude $|H(j\omega)|$ equals the *reciprocal of the distance* from the point $j\omega$ on the imaginary axis to the pole at $s = -1/RC$. As $\omega \to 0$, the distance is small and $|H|$ is large; as $\omega \to \infty$, the distance grows and $|H| \to 0$.

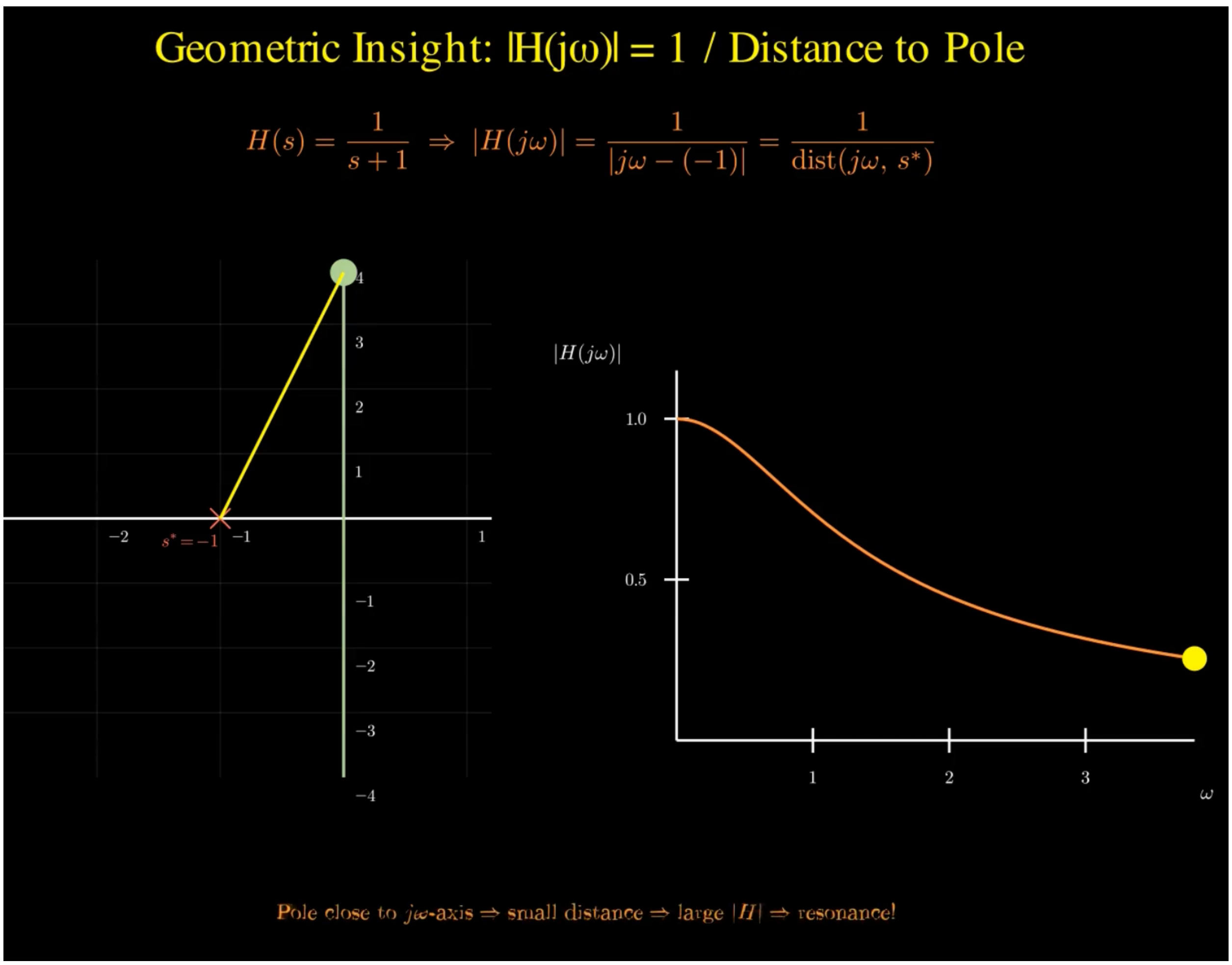

Figure 1: RC circuit pole-zero map. The distance from $j\omega$ to the pole at $s = -1/RC$ equals $1/|H(j\omega)|$.

4 Forced Mass-Spring Oscillator

4.1 The Second-Order ODE

A mass on a spring with damping and a cosine forcing term obeys

$$x'' + 2a\,x' + \omega_n^2\,x = F_0\cos(\omega_f t), \tag{8}$$

where a is the decay rate, $\omega_n = \sqrt{k/m}$ is the natural frequency, ω_f is the forcing frequency, and F_0 is the forcing amplitude. The system constants used in this project are $a = 0.70$, $\omega_d = 2.50$, $\omega_f = 2.00$, $F_0 = 3.0$, giving $\omega_n = \sqrt{a^2 + \omega_d^2} \approx 2.596$ and damping ratio $\zeta = a/\omega_n \approx 0.270$ (underdamped).

4.2 Laplace Transform of the ODE

Applying the Laplace transform with initial conditions $x(0) = x_0$, $x'(0) = v_0$:

$$\left(s^2 + 2as + \omega_n^2\right) X(s) = \frac{F_0\,s}{s^2 + \omega_f^2} + \left[s\,x_0 + v_0 + 2a\,x_0\right]. \tag{9}$$

The right-hand side separates cleanly: the first term is due to the forcing, the second to initial conditions. Solving for $X(s)$:

$$X(s) = \underbrace{\frac{F_0\,s}{\left(s^2 + \omega_f^2\right)\left(s^2 + 2as + \omega_n^2\right)}}_{X_p(s)} + \underbrace{\frac{s\,x_0 + v_0 + 2a\,x_0}{s^2 + 2as + \omega_n^2}}_{X_h(s)}. \tag{10}$$

4.3 Time-Domain Decomposition

Inverting each part separately:

$$x_h(t) = e^{-at}[A\cos(\omega_d t) + B\sin(\omega_d t)]\,, \tag{11}$$

$$x_p(t) = |H(j\omega_f)|\cos(\omega_f t + \angle H(j\omega_f))\,, \tag{12}$$

where A and B are determined by matching initial conditions, and $H(j\omega_f) = \omega_n^2/\left[(\omega_n^2 - \omega_f^2) + 2ja\omega_f\right]$ is the system's frequency response evaluated at the forcing frequency. The transient $x_h(t)$ decays at rate e^{-at}; the particular solution $x_p(t)$ persists indefinitely.

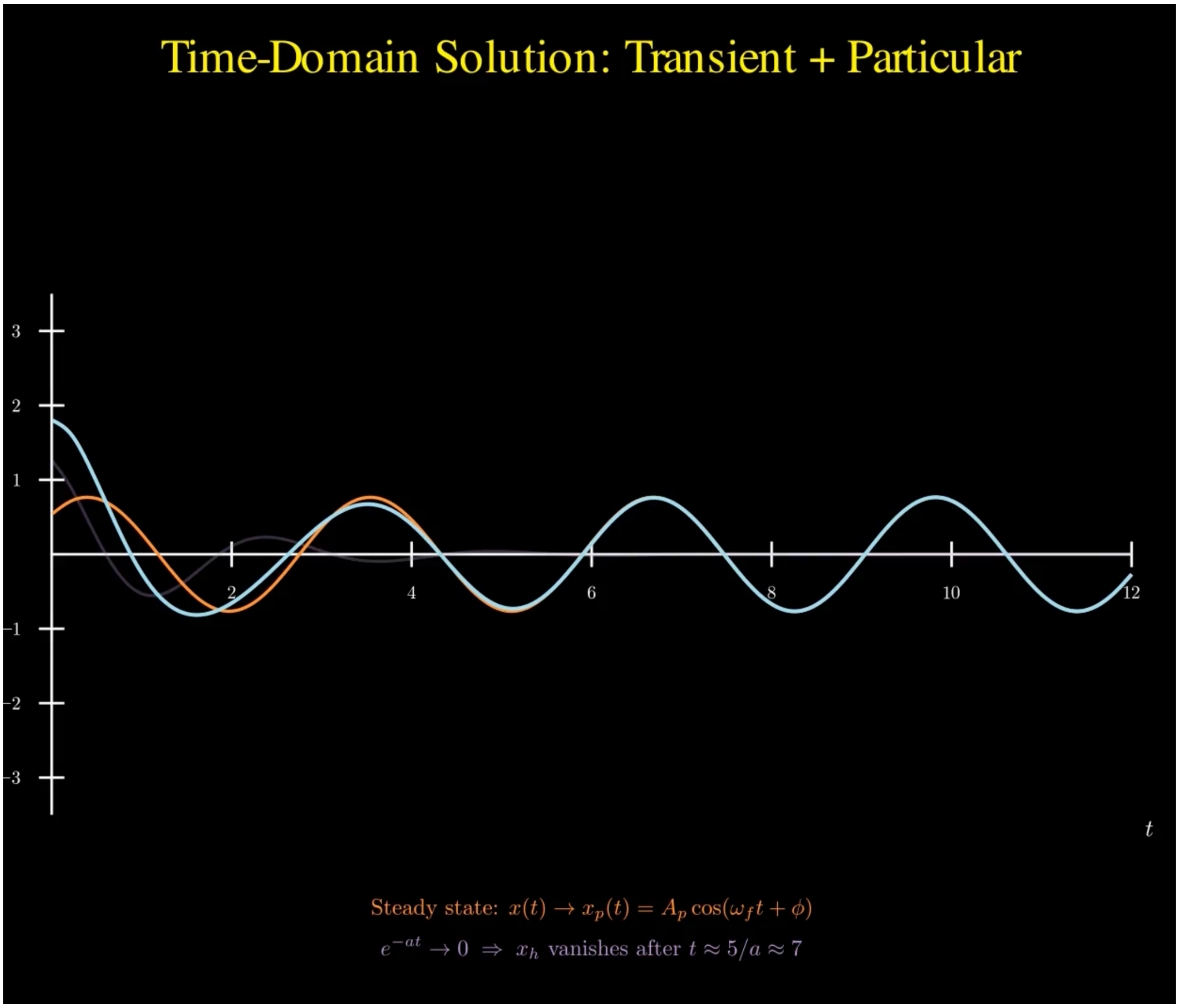

Figure 2: Time-domain decomposition: transient $x_h(t)$ (purple), particular $x_p(t)$ (orange), and total $x(t)$ (blue).

4.4 Frequency Response and Resonance

The amplitude of the steady-state response is

$$|H(j\omega)| = \frac{\omega_n^2}{\sqrt{(\omega_n^2 - \omega^2)^2 + (2a\omega)^2}}, \tag{13}$$

which peaks at the resonance frequency

$$\omega_r = \sqrt{\omega_n^2 - 2a^2} \approx 2.401. \tag{14}$$

As $a \to 0$ (less damping), $\omega_r \to \omega_n$ and the peak height $\to \infty$: pure resonance.

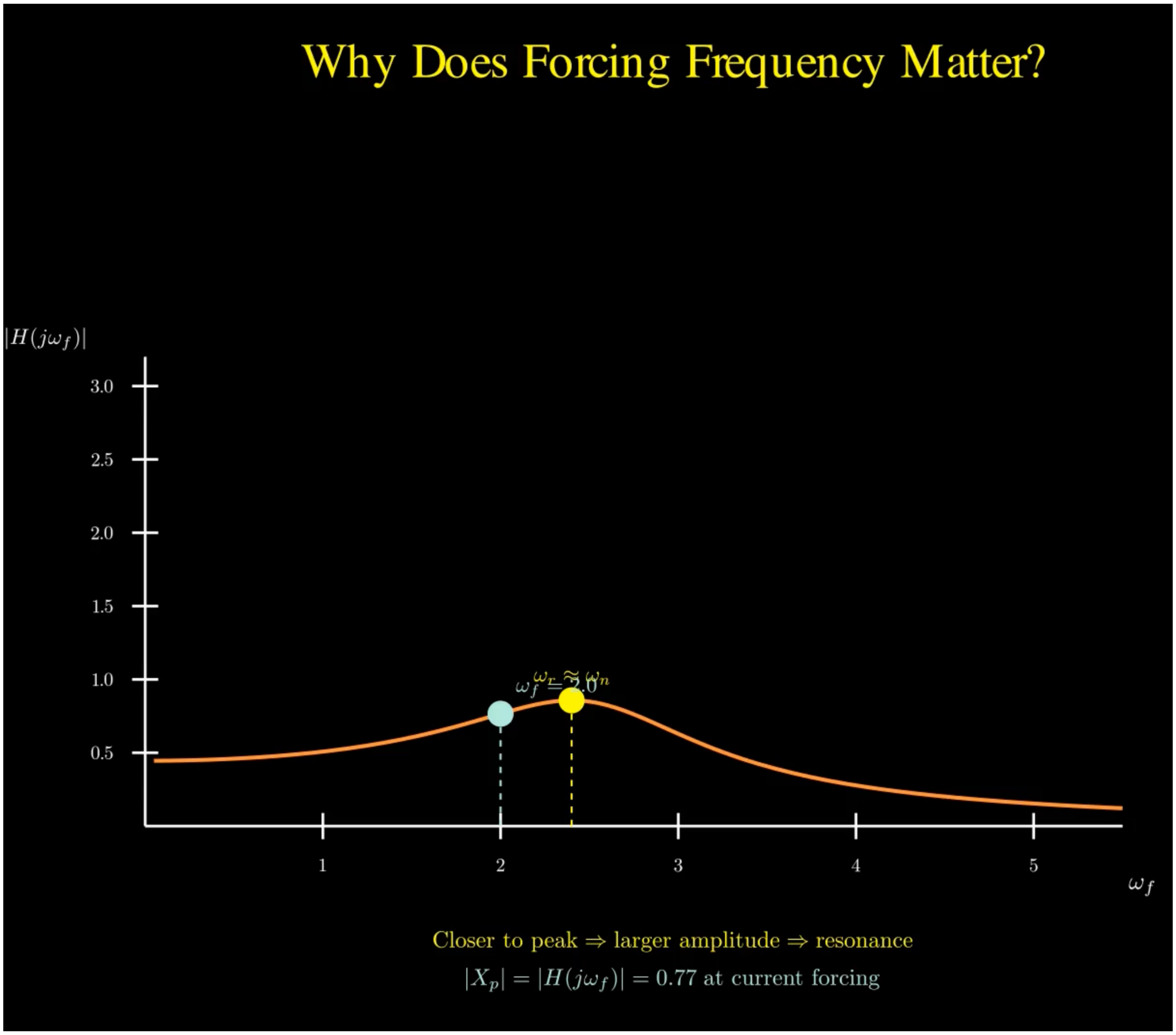

Figure 3: Frequency response $|H(j\omega)|$ with resonance peak at $\omega_r \approx 2.401$ annotated.

4.5 Pole-Zero Map

The system poles are at $s = -a \pm j\omega_d$, the forcing poles at $s = \pm j\omega_f$, and an initial-condition zero at $s = -2a$. Key geometric relationships read directly off the pole locations:

- Decay rate: $a = -\text{Re(pole)}$
- Damped frequency: $\omega_d = \text{Im(pole)}$
- Natural frequency: $\omega_n = |\text{pole}|$ (distance from origin)
- Damping ratio: $\zeta = \cos\theta$ where θ is the angle from the negative real axis
- Resonance gap: $\Delta\omega = \omega_d - \omega_f$ (proximity drives amplitude)

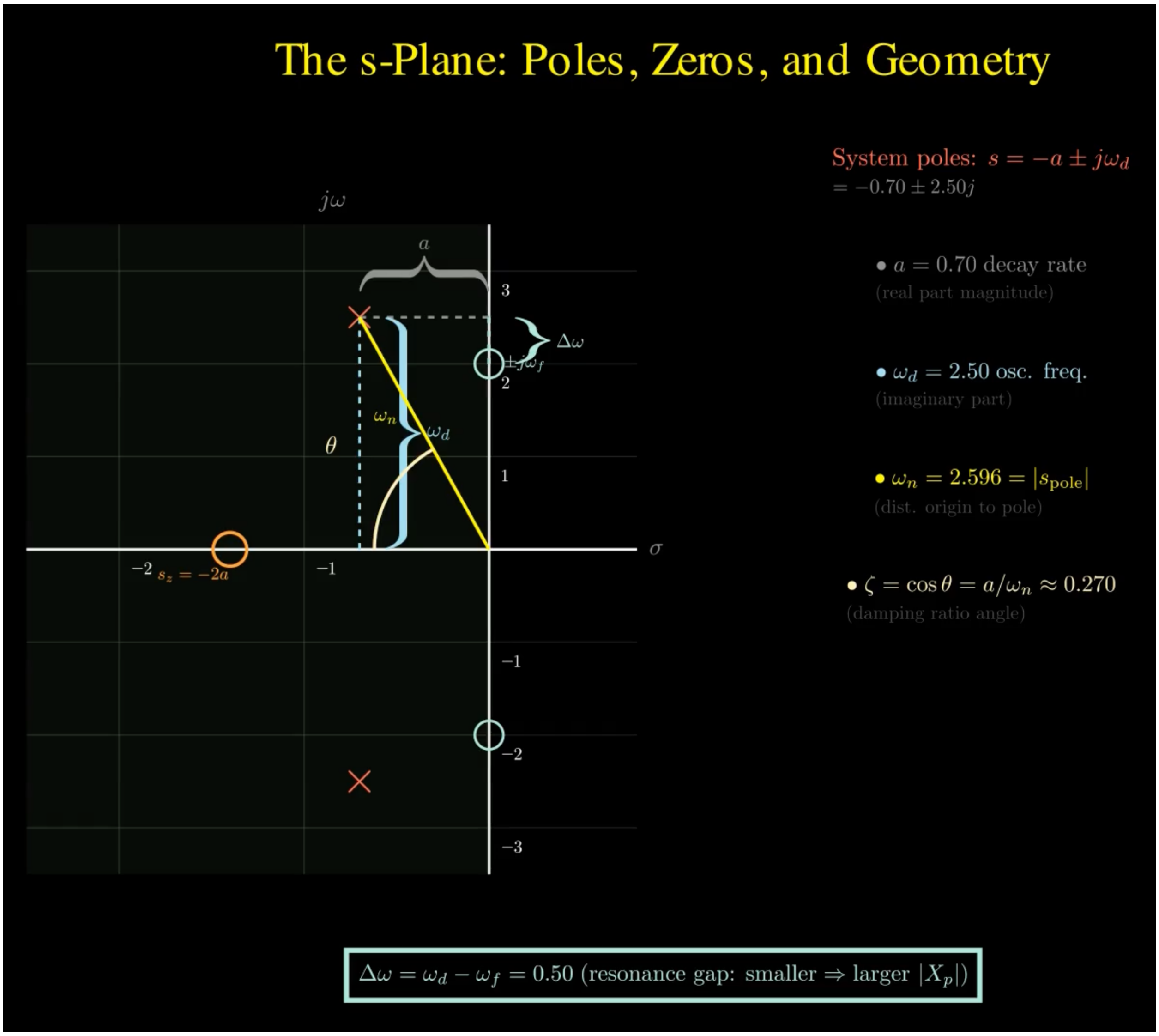

Figure 4: Pole-zero map showing system poles (×), forcing poles (○), IC zero, damping angle θ, and resonance gap $\Delta\omega$.

5 The $|H(s)|$ Surface in 3D

5.1 Visualizing the Transfer Function

The transfer function $H(s) = \omega_n^2/(s^2 + 2as + \omega_n^2)$ is a complex-valued function of $s = \sigma + j\omega$. Plotting $|H(\sigma + j\omega)|$ as a height over the complex plane produces a surface with spikes (poles) and valleys, directly revealing the system's behavior. Evaluating on the imaginary axis ($\sigma = 0$) gives the Bode magnitude plot as a one-dimensional slice of this surface.

5.2 Four Damping Cases

The shape of the surface changes dramatically with the damping ratio ζ:

- **Undamped** ($\zeta = 0$): Poles on the $j\omega$ axis; the surface has infinite spikes at $\pm j\omega_n$. Any sustained forcing at ω_n causes unbounded growth.
- **Underdamped** ($\zeta \approx 0.27$): Complex conjugate poles in the left half-plane. The surface has two sharp (but finite) peaks near the imaginary axis.
- **Critically damped** ($\zeta = 1$): A repeated real pole at $s = -\omega_n$. The surface has one broad, symmetric mound with no oscillatory peak.
- **Overdamped** ($\zeta = 1.5$): Two distinct real poles. The surface splits into two separate bumps along the negative real axis.

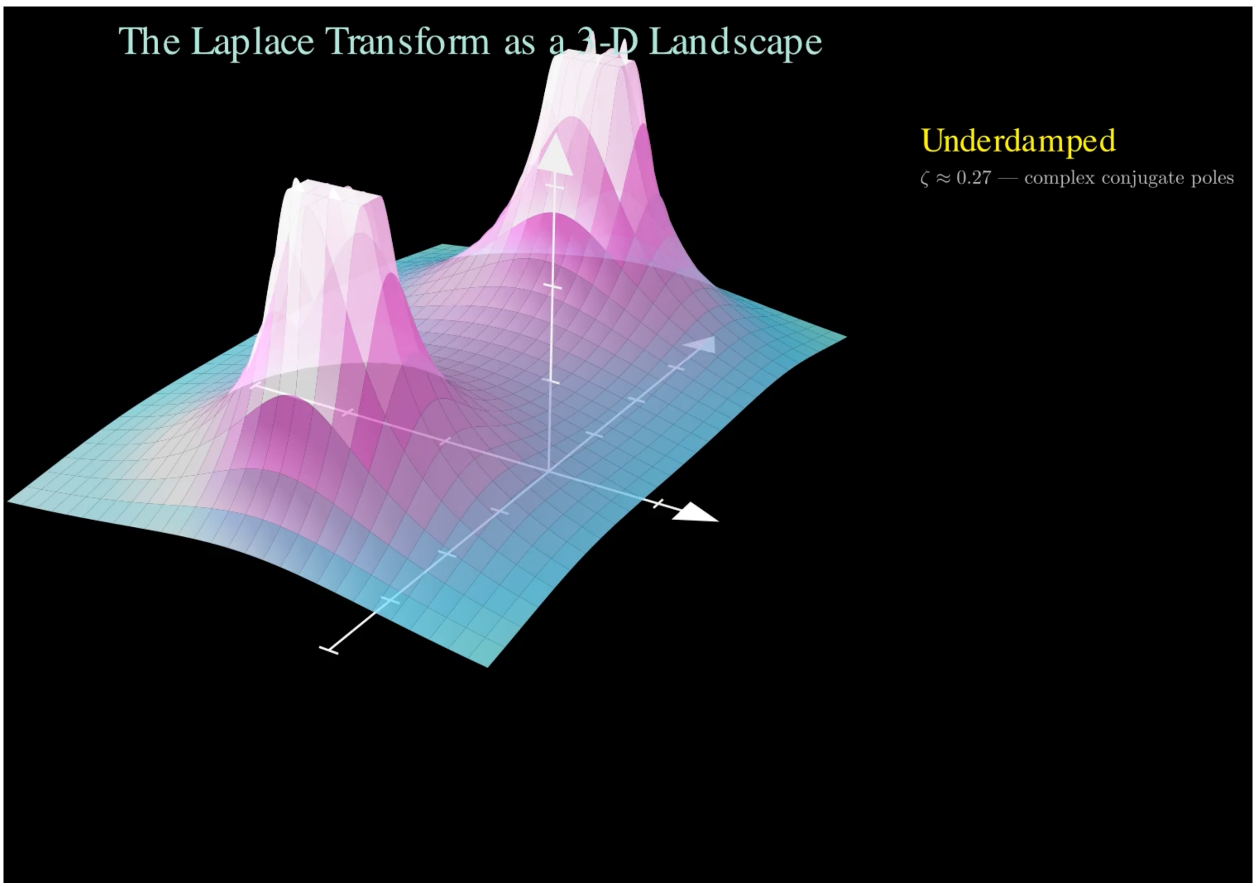

Figure 5: The $|H(s)|$ surface for all four damping cases: undamped ($\zeta = 0$), underdamped ($\zeta \approx 0.27$), critically damped ($\zeta = 1$), and overdamped ($\zeta = 1.5$).

5.3 Three-Surface Decomposition

Just as $X(s) = X_h(s) + X_p(s)$ in the algebraic domain, the three-dimensional visualization shows three overlaid surfaces:

- $|X_h(s)|$: Transient surface – spikes at the system poles $s = -a \pm j\omega_d$, governed by initial conditions and system damping.
- $|X_p(s)|$: Forced surface – spikes at the forcing poles $s = \pm j\omega_f$, scaled by F_0 and the system's gain at ω_f.
- $|X(s)|$: Combined – the superposition, with peaks at both sets of poles.

The resonance effect becomes geometrically clear: as ω_f approaches ω_d, the forcing poles slide toward the system poles, and the two surfaces merge into a single enormous spike.

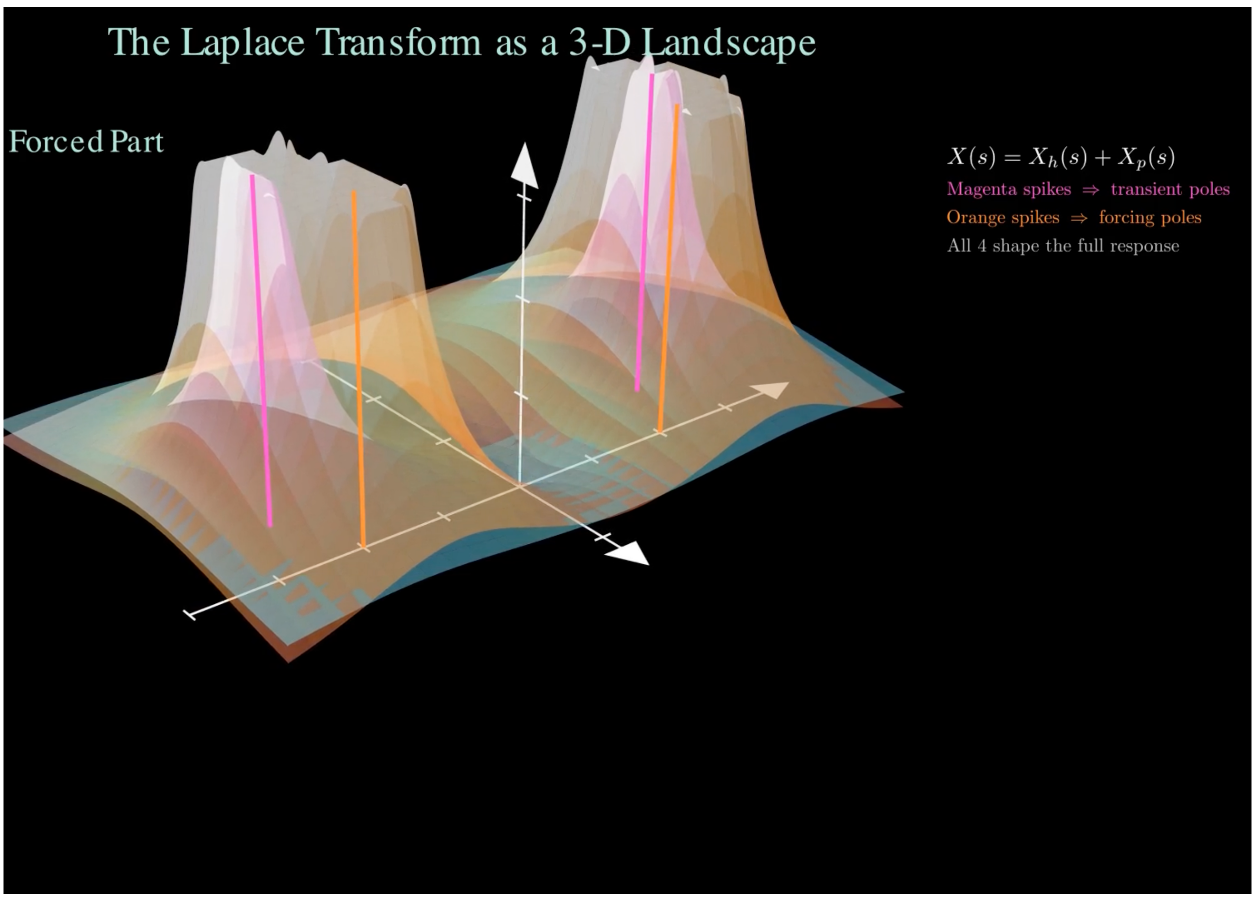

Figure 6: Three-surface decomposition: transient $|X_h(s)|$ (teal), forced $|X_p(s)|$ (orange), and combined $|X(s)|$ overlaid.

6 The Weighted-Area Interpretation

An important visual motivates the definition of the Laplace transform. Consider $f(t) = e^{-at}\cos(\omega_d t)$, the impulse response of the underdamped system. For a fixed σ, the integrand $f(t) \cdot e^{-\sigma t}$ is a damped oscillation. The Laplace transform $F(\sigma)$ equals the net signed area under this curve – the "weighted area" – as σ varies. This is visualized as a 2D surface $z(t, \sigma) = f(t) \cdot e^{-\sigma t}$, where integrating along the t-axis for each σ traces out the transform.

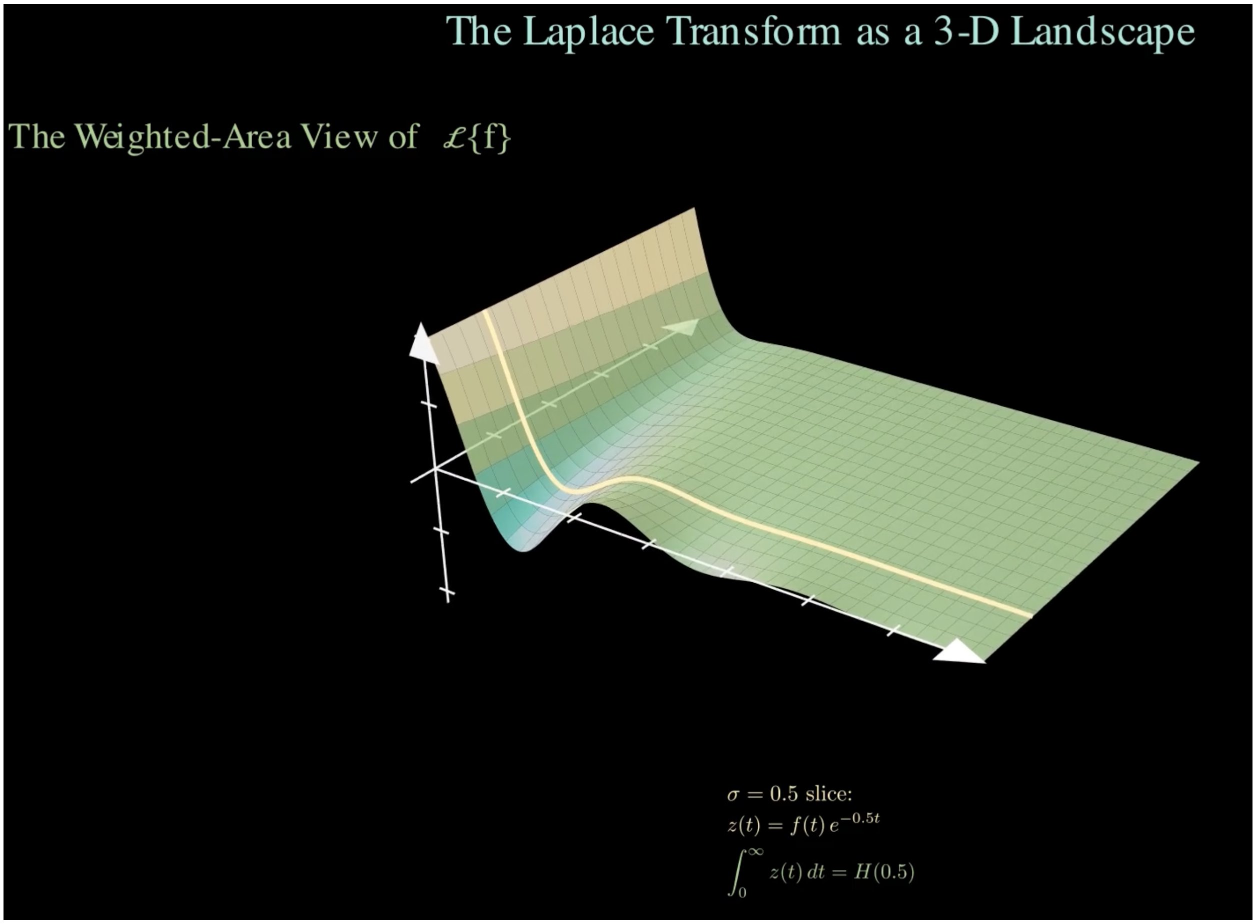

Figure 7: Weighted-area surface $z(t, \sigma) = f(t) \cdot e^{-\sigma t}$. Integrating each σ-slice traces out the Laplace transform.

7 Conclusion

This project demonstrates that the Laplace transform is not merely an algebraic trick but a geometric one: moving to the complex s-plane turns the behavior of a physical system into a visible landscape. Poles mark the natural resonances of the system; their distance from the imaginary axis measures stability; their proximity to a forcing frequency determines amplification. Three animated videos were produced to make these ideas accessible from first principles, progressing from the single-pole RC circuit to the full three-surface decomposition of a forced oscillator. The visualizations were built using the Manim animation library (Python), with all surface formulas derived analytically and verified numerically.

References

[1] R. Nave, "Novel 3D Visualization of Laplace and Fourier Transforms," *Trends in Technical & Scientific Research*, vol. 1, no. 1, 2018. `https://juniperpublishers.com/ttsr/pdf/TTSR.MS.ID.555558.pdf`

[2] T. Donahue, "Motivating the Definition of the Laplace Transform," *CODEE Journal*, vol. 6, 2009. `https://scholarship.claremont.edu/cgi/viewcontent.cgi?article=1009&context=codee`

[3] 3Blue1Brown, "Why Laplace Transforms are Useful," YouTube, 2023. `https://www.youtube.com/watch?v=n2y7n6TVE5E`

[4] 3Blue1Brown, "The Physics of Euler's Formula," YouTube, 2017. `https://www.youtube.com/watch?v=mvmuCPvVSWQ`

[5] Manim Community, *Manim – Mathematical Animation Engine*. `https://www.manim.community`, 2024.

[6] University of Washington, *Washington eXperimental Mathematics Lab (WXML) Project Showcase*. `https://wxml.math.washington.edu`, 2026.